ACS APPLIED MATERIALS & INTERFACES

www.acsami.org

Research Article

Organophilicity of Graphene Oxide for Enhanced Wettability of ZnO Nanorods

Pavan S. Emani,[⊥] Hisham A. Maddah,[⊥] Arjun Rangoonwala, Songwei Che, Aditya Prajapati, Meenesh R. Singh, Dieter M. Gruen,* Vikas Berry,* and Sanjay K. Behura*

Cite This: *ACS Appl. Mater. Interfaces* 2020, 12, 39772–39780

Read Online

ACCESS | Metrics & More | Article Recommendations | Supporting Information

ABSTRACT: Interfacing two-dimensional graphene oxide (GO) platelets with one-dimensional zinc oxide nanorods (ZnO) would create mixed-dimensional heterostructures suitable for modern optoelectronic devices. However, there remains a lack in understanding of interfacial chemistry and wettability in GO-coated ZnO nanorods heterostructures. Here, we propose a hydroxyl-based dissociation-exchange mechanism to understand interfacial interactions responsible for GO adsorption onto ZnO nanorods hydrophobic substrates. The proposed mechanism initiated from mixing GO suspensions with various organics would allow us to overcome the poor wettability ($\theta \sim 140.5°$) of the superhydrophobic ZnO nanorods to the drop-casted GO. The addition of different classes of organics into the relatively high pH GO suspension with a volumetric ratio of 1:3 (organic-to-GO) is believed to introduce free radicals (−OH and −COOH), which consequently result in enhancing adhesion (chemisorption) between ZnO nanorods and GO platelets. The wettability study shows as high as 75% reduction in the contact angle ($\theta = 35.5°$) when the GO suspension is mixed with alcohols (*e.g.*, ethanol) prior to interfacing with ZnO nanorods. The interfacial chemistry developed here brings forth a scalable tool for designing graphene-coated ZnO heterojunctions for photovoltaics, photocatalysis, biosensors, and UV detectors.

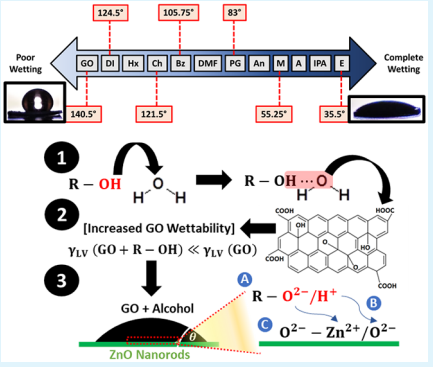

KEYWORDS: *2D materials, mixed-dimensional heterostructure, interfacial chemistry, wettability*

INTRODUCTION

Designing mixed-dimensional heterostructures[1−4] by interfacing two-dimensional (2D) graphene oxide (GO) layers with one-dimensional (1D) zinc oxide (ZnO) nanorods is paramount to the understanding of existing dipolar van der Waals interactions and interfacial charge carrier transport. Interfacing GO with ZnO nanorods creates mixed-dimensional 2D/1D heterostructures with potential applications in biosensors,[5−7] UV detectors,[8,9] dye-sensitized solar cells,[10−12] perovskite tandem cells,[13−15] and catalysis.[16,17] Conventionally, GO/ZnO nanocomposites are fabricated by either chemical vapor deposition,[3,18] spray pyrolysis,[19,20] spin-coating[21] methods, and/or *via* the traditional drop-casting technique[22,23] of GO on a hydrothermally grown ZnO substrate. However, ZnO nanorods are extremely hydrophobic in nature, posing challenges toward effective and uniform coating of GO layers presynthesized in water-based suspensions *via* the Hummers method.[24] ZnO surface hydrophobicity and wettability to GO layers can be explained *via* interfacial phenomena that need to be understood from the interactions between solids (ZnO), liquids (GO suspension), and vapors (air), as explained in detail in the Supporting Information (Section S1).[24] A contact angle of 167° was measured earlier for a water droplet on ZnO nanorods, indicating the superhydrophobic nature of ZnO substrates.[24] The high ZnO hydrophobicity is explained by the trapped layers of air between the nanorods, consequently applying an opposing force against the desired interfacial adhesion. Another reason for the poor wettability of ZnO nanorods is due to the lack of hydroxyl (−OH) groups at the nanorod surface.[24] Interestingly, it has been found that both ZnO morphology and surface coverage density allow the tunability of ZnO hydrophobicity.[25] Earlier studies indicated that ZnO hydrophobicity increases with both coverage density and surface area of created nanorods.[25−27] On the contrary, thin-film ZnO nanostructures with minimum coverage density show low water-droplet contact angles.[25−27] Moreover, exposing ZnO nanorods to UV radiation leads to unusual wettability characteristics and superhydrophilic nature,[25,26] while thermal annealing of ZnO nanorods after UV exposure results in recurrence of the hydrophobic properties.[27]

Interfacing GO nanosheets (suspended in water) with solid-state ZnO nanorods requires a comprehensive understanding of the possible interfacial interactions. In general, GO

Received: May 25, 2020
Accepted: August 3, 2020
Published: August 3, 2020

https://dx.doi.org/10.1021/acsami.0c09559
ACS Appl. Mater. Interfaces 2020, 12, 39772−39780

nanosheets become hydrophilic in the presence of numerous hydrogen bond interactions with water (or organic) molecules existing in the GO−water (or GO−water/organic) suspension.[28] Despite that, pristine graphene is known to be hydrophobic in nature due to the absence of edge −OH groups for water attraction.[29,30] It has been determined that introducing vacancy defects onto the GO surface would result in decreasing GO wettability.[28] To achieve high ZnO hydrophilicity for GO−water, we should have either a low surface tension liquid or high surface energy solid achieved by: (i) low liquid−vapor surface tension (γ_{LV}) and/or (ii) high solid−vapor surface energy (γ_{SV}).[31−33] This work considered the addition of organics to reduce γ_{LV} of GO−water. The same conditions are believed to be also true for achieving high GO hydrophilicity in water suspensions, as a prerequisite for high wettability of ZnO for GO−water. Detailed explanations on the concentration dependency of GO wettability and the impact of solution pH and hydroxyl groups on the wettability characteristics and mechanisms of GO in water are presented in the Supporting Information (Section S2).[29] High GO wettability in water is necessary for high ZnO wettability to GO, which are both achieved by adding organics to have GO−water/organic mixtures containing the desired hydroxyl groups. Thus, we need to have a comprehensive understanding of the interfacial chemistry, ZnO morphology, pH dependency, GO concentrations, and wetting mechanisms for enhanced chemisorption and possibility to obtain GO-coated-ZnO nanorods heterostructures.

Herein, we propose a hydroxyl-based dissociation-exchange mechanism that would allow us to overcome the superhydrophobic nature and poor wettability of ZnO nanorods to drop-casted GO layers suspended in water. Ten organic media have been chosen for dispersing GO−water suspension and these organics were mixed with presynthesized GO−water suspension in a volumetric ratio of 1:3 (organic-to-GO). The resultant (GO−water/organic) mixtures are believed to enhance ZnO/GO interactions and thereby forming the heterostructure. The strength of the interfacial interactions and ZnO wettability characteristics have been studied through analyzing ZnO substrate work of adhesion, GO/organic contact angle, and the hypothesized interfacial chemistry mechanisms.

EXPERIMENTAL METHODS AND MODELS

Growth and Characterization of ZnO Nanorods and GO-Coated ZnO Nanorods Heterostructure. ZnO nanorods are synthesized hydrothermally on a zinc substrate following the hydrothermal growth method reported elsewhere.[34−36] Mechanisms of ZnO nucleation and growth of nanorods have been previously studied to optimize the nanorods aspect ratio (length-to-diameter), orientation, and surface coverage (density).[34−36] The detailed experimental methods for the preparation of the Zn foil substrate and the hydrothermal growth solution for ZnO nanorods are presented in the Materials and methods section. The five-step process describing the reaction mechanisms involved in the growth and synthesis of ZnO nanorods[37] is presented in the Supporting Information (Section S3).

Prepared ZnO nanorods and GO-coated ZnO nanorods samples were characterized *via* field-emission scanning electron microscopy (FESEM) and confocal Raman spectroscopy (WITec alpha 300 RA, laser excitation of 532 nm). ZnO nanorods can be clearly seen from FESEM morphology images shown in Figure 1b,c. The nanorods are of ∼8−10 μm in length and ∼0.3−0.4 μm in width (diameter), indicating an approximated average aspect ratio of ∼26. Here, a combination of vertically aligned (thin nanorods) and horizontally aligned (thick nanorods) ZnO nanorods are nucleated. Furthermore, ZnO nanorods exhibited Raman vibrational modes E_2^{Low}, E_2^{High}, A_1(LO), and A_1(2LO) at 95, 434, 564, and 1134 cm^{-1}, respectively, as shown in Figure 2a with variations in observed intensities.[38−40] The E_2^{Low} and E_2^{High} peaks appear from in-plane longitudinal vibrations of Zn and O atoms, while A_1(LO) and A_1(2LO) bands occur from out-of-plane transverse vibrations.[38]

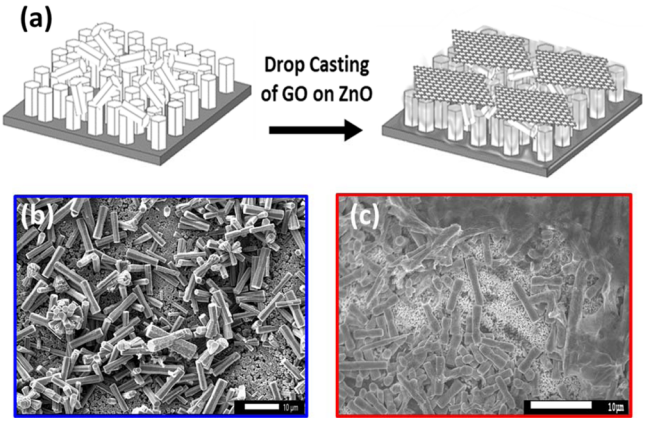

Figure 1. Synthesis of ZnO nanorods: (a) 3D schematic illustrating the synthesized ZnO nanorods on Zn foil followed by drop-casting of GO suspensions showing GO coating and deposition on and/or around the ZnO nanorods; (b,c) FESEM images of the hydrothermally grown ZnO nanorods before and after being interfaced with GO, respectively. A combination of vertically and horizontally oriented ZnO nanorods are formed (b) which are then covered with GO layers (c).

Next, the GO suspension was synthesized by chemical exfoliation of graphite flakes *via* the Hummers method and then dialyzed in deionized (DI) water. This allows producing low acidity (pH ∼ 6) pure GO−water suspensions which were further mixed with various organics for GO−water/organic mixtures. The detailed experimental methods for the synthesis of GO are presented in the Materials and Methods section. The resultant GO−water/organic suspensions were then drop-casted on the ZnO nanorods superhydrophobic surface, as shown in Figure 1a, and then left to dry overnight. The GO-coated ZnO heterostructures are confirmed from the coated semitransparent layer of GO atop and around ZnO nanorods shown in Figure 1c. The ZnO nanorods are wrapped by GO forming GO-coated ZnO nanorods heterostructures as seen by the presence of both ZnO and GO atomic Raman vibrational mode signatures illustrated in Figure 2b. Raman characterization of the ZnO/GO heterostructures drop-casted with GO−water mixed with different organics can be found in the Supporting Information (Figure S3). Most importantly, graphene is observed in Figure 2b from: (i) the graphitic structural defects and disordered sp^2 domains (D band at 1352 cm^{-1}) and (ii) the graphitic vibrations of sp^2-hybridized C=C bonds (G band at 1596 cm^{-1}).[41−44]

Models and Equations. Young's equation,[45] as in eq 1, describes the condition of equilibria when a drop of liquid is drop-casted on a smooth solid surface. Involved surface energies, including γ_{SV}, liquid−solid surface energy (γ_{LS}), and γ_{LV} can be associated with the measured Young contact angle (θ) to understand the hydrophobicity between solids and liquids and/or to measure the effect of surface roughness factor (r) on the contact between rough surfaces and liquids (*e.g.*, water).[26] Because we propose using various hydrocarbon (HC)-based organics for the purpose of reducing hydrophobicity of ZnO nanorods to GO, we may use the approximated equation, as shown in eq 2, for the calculation of the overall γ_{LV} from surface energies of both GO and the involved HC medium and their selected volume fractions; also from γ_{GO} and γ_{HC} which correspond to liquid−air surface tensions of the GO and organic solvents, respectively, as presented in the Supporting Information (Section S4). The selected organic media along with their expected liquid−vapor surface energies

https://dx.doi.org/10.1021/acsami.0c09559
ACS Appl. Mater. Interfaces 2020, 12, 39772−39780

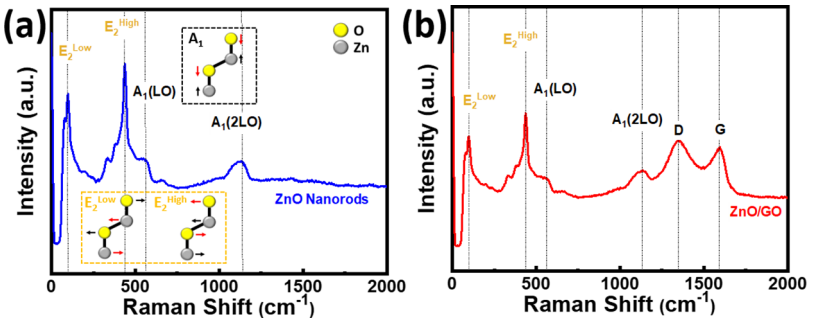

Figure 2. Raman spectroscopy analysis of the synthesized (a) ZnO nanorods films and (b) GO-coated ZnO nanorods heterostructures from drop-casting GO suspensions, and the inset in (a) shows both in-plane (E_2) and out-of-plane (A_1) vibrational modes occurring in the ZnO lattice.

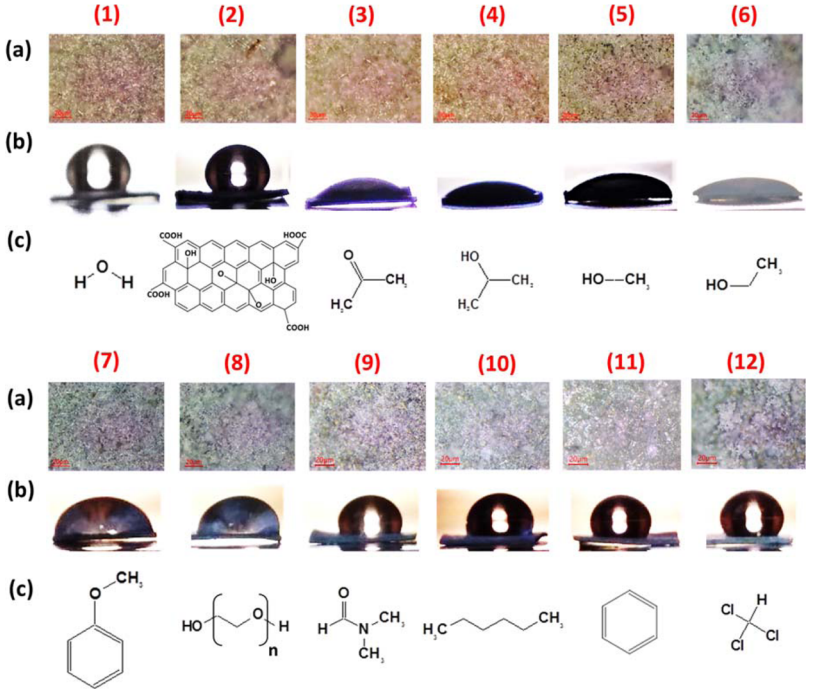

Figure 3. (a) Optical microscope images; (b) contact angle of the drop-casted GO on ZnO nanorods substrates; (c) chemical structure of the used organic media (if any used with GO as in sample number 3 to 12 from Table 1), where numbers refer to (1) DI water; (2) GO; (3) acetone; (4) isopropyl alcohol (IPA); (5) methanol; (6) ethanol; (7) anisol; (8) PG; (9) DMF; (10) hexane; (11) benzene; and (12) chloroform.

are reported in Table S2 in the Supporting Information. Moreover, the Young–Dupré model[31] from eq 3 is used to obtain the liquid/solid adhesion energy per unit area (W_{LS}), that is, the amount of work released per unit area when adhesion occurs. For example, more work of adhesion is preferred for lower contact angles at the GO/ZnO interface, thus increasing wettability by lowering hydrophobic characteristics of ZnO.

$$\gamma_{SV} - \gamma_{LS} = \gamma_{LV} \cos\theta \quad (1)$$

$$\gamma_{LV} \approx x\gamma_{GO} + (1 - x)\gamma_{HC} \quad (2)$$

$$W_{LS} = \gamma_{LV}(1 + \cos\theta) \quad (3)$$

Determination of the contact angles between GO (liquid) and ZnO nanorods (solid substrate) using various organic media mixed with GO (to lower its hydrophobicity and improve wettability) will help us in establishing the critical surface tension (γ_c) at the GO/ZnO interface.[46] Having various concentrations of organics mixed with GO liquid would modify GO wettability properties from the introduced functional groups (*e.g.*, =O, −OH, and −COOH) which are found to be hydrophilic in nature. The Fox–Zisman linear approximation in eq 4 is used to calculate the γ_c value at ($\gamma_{LV} = \gamma_{SV}$ and $\gamma_{LS} = 0$) which implies that $\cos\theta = 1$ (the maximum wettability occurs at $\theta = 0$). Writing eq 4 in terms of γ_c, as shown in eq 5, and fitting the data generated from the organic media used in the GO/ZnO wettability test by using linear regression analysis allow us to determine the optimal HC media for highest wettability. Any liquid with surface tension below the critical surface tension ($\gamma_{LV} < \gamma_c$) would completely wet the ZnO solid surface at $\theta = 0$ that can be approximated from the Zisman model.[46−49] However, the complete wetting case might not be possible to achieve; hence, selecting the closest γ_{LV} to γ_c is the ideal way of choosing the optimum medium for enhancing wettability. In short, Zisman equation describes that if $\gamma_{SV} > \gamma_{LS}$, then $\cos\theta$ will be positive, indicating that $\theta < 90$ and wetting occurs (from either high γ_{SV} and/or low γ_{LV} as methanol and ethanol); similarly, if $\gamma_{SV} < \gamma_{LS}$, then $\cos\theta$ will be negative, resulting in $\theta > 90$ and dewetting occurs (from either low γ_{SV} and/or high γ_{LV} as water). Because $\gamma_c = \gamma_{SV}$ (only if $\gamma_{LS} = 0$ at $\theta = 0 \rightarrow \gamma_{LV} = \gamma_{SV}$), we can rewrite eq 4 in terms of liquid–vapor tensions only to reach a complete wetting case, as shown in eq 5, which explains that it is only possible to have complete wetting when $\gamma_{LV} \rightarrow \gamma_c$ and $\cos\theta = 1$.[50]

$$\cos\theta \approx \left(\frac{\gamma_{SV} - \gamma_{LS}}{\gamma_{LV}}\right) \quad (4)$$

https://dx.doi.org/10.1021/acsami.0c09559
ACS Appl. Mater. Interfaces 2020, 12, 39772−39780

$$\cos\theta \approx 1 - \left(\frac{\gamma_{LV} - \gamma_c}{\gamma_{LV}}\right) \quad (5)$$

RESULTS AND DISCUSSION

Contact angle measurements were carefully obtained from the taken photographs (Figure 3) using two image processing software (Snip/Sketch and ImageJ[51]), as shown in Table 1.

Table 1. Calculated Contact Angles Using Two Common Software for the Wettability of ZnO Surfaces to DI, GO, and GO/HC Mixtures at 25 °C

		contact angle (deg); image processing software			
S/N	material[a]	Snip/Sketch	ImageJ	ImageJ fitting	averaged contact angle (deg)
1	DI	127	122	circle-fit	124.5 ± 3
2	GO	132	149	ellipse-fit	140.5 ± 8
3	GO−A	42.5	48	manual-fit	45.25 ± 3
4	GO−IPA	36.5	50	manual-fit	43.25 ± 7
5	GO−M	57.5	53	manual-fit	55.25 ± 2
6	GO−E	34	37	manual-fit	35.5 ± 2
7	GO−An	79.5	68	circle-fit	73.75 ± 5
8	GO−PG	85	81	circle-fit	83 ± 3
9	GO−DMF	109	101	circle-fit	105 ± 4
10	GO−Hx	117.5	94	circle-fit	105.75 ± 9
11	GO−Bz	113.5	130	ellipse-fit	121.75 ± 8
12	GO−Ch	122	121	circle-fit	121.5 ± 1

[a]DI: deionized water; GO: graphene oxide suspension; A: acetone; IPA: isopropyl alcohol; M: methanol; ethanol; An: anisole; PG: polyethylene glycol; DMF: dimethyl formamide; Hx: hexane; Bz: benzene; and Ch: chloroform.

Measurement methods are briefly discussed in the Supporting Information (Section S4). We averaged the determined angles for DI, GO, and GO/HC mixtures to have more accurate results. Optical microscope images have been taken for the different GO/ZnO samples using the optical microscope (AmScope MX6R) after drop-casting and overnight drying in ambient conditions.

The designed contact angle apparatus illustrated in the Supporting Information (Figure S2) was utilized to take photos of the drop-casted GO−water and GO−water/organic suspensions on ZnO nanorods for wettability analysis. Each sample of ZnO nanorods was synthesized under the same conditions, hence warranting the use of the Young−Dupre model to determine surface tensions and work of adhesion. The inverse relationship between $(\gamma_{SV} - \gamma_{LS})$ and $\cos\theta$ can be shown in Figure 4a. In samples containing pure GO, the contact angle was greater than 90°, resulting in a negative value for $(\gamma_{SV} - \gamma_{LS})$, whereas the samples with a contact angle less than 90° results in a positive value for $(\gamma_{SV} - \gamma_{LS})$, which is justified by Young's equation as in eq 1.

Enhanced wettability may arise from a decrease in γ_{LS} or γ_{LV} and possibly an increase in γ_{SV}. GO has a liquid−vapor surface energy of 62.1 mN/m. A few selected organics mixed with GO enhanced wettability owing to the presence of hydroxyl −OH radicals. The added hydroxyl groups create strong hydrogen bond interactions at the water interface for water attraction.[28] The results, as shown in Figure 4b, indicate a reduction in liquid−vapor surface tension as compared to the GO suspension (γ_{LV} = 62.1 mN/m, Table S2) because of the presence of organic functional groups. The symmetry between work of adhesion (W_{LS}) and contact angle (Figure 4c,d) is evident and can be validated from the inverse relationship between the two parameters. A critical surface tension of γ_c = 47 mN/m is estimated to achieve a complete wettability of ZnO nanorods to GO, as illustrated in Figure 4e. When more work of adhesion is released from a liquid drop wetting a solid substrate, this energy will be enough to overcome cohesion within the GO−water suspension and thereby enhance ZnO wettability for GO−water. GO/DMF, GO/hexane, GO/benzene, and GO/chloroform showed poor wettability on ZnO nanorods (θ > 100°). The poor wettability from these mixtures might be due to the presence of hydrophobic single-bond oxygen atoms and/or long HCs or aromatic chains, as shown in Figure 3. Moreover, the poor wettability observed for GO−water/PG might be due the chemical purity of only 50% for PG mixed with water as well as the high value of γ_{LV} = 76.1 mN/m (Table S2). We believe that introducing molecules with only −OH or =O groups is the ideal case because (3), (4), (5), and (6) in Figure 3c show the highest wettability as compared to (8), (9), (10), and (11); keeping in mind that long aliphatic or cyclic HCs are expected to result in poor wettability regardless of existing groups. Conversely, low contact angles (θ < 80°) were observed for GO−acetone, GO−IPA, GO−methanol, GO−ethanol, GO−anisole, and with highest wettability reserved for GO−ethanol ($\theta \approx$ 35°).

As expected, the ZnO surface seems to be very hydrophobic to GO−water, but with obvious reduction in contact angle and hydrophobicity, once ethanol, acetone, or IPA was added to GO−water suspensions. We have measured the sliding angle using DI, GO−water, GO−water/acetone, and GO−water/IPA mixtures (mixtures in a 1:3 volumetric ratio of organic-to-GO). However, we found that the superhydrophobic ZnO nanorods surface is characterized with a strong adhesion of the liquid drop to an extent that would not make it possible to measure the sliding angle. This is because the surface does not allow drops to slide down on the surface under the gravity effect. We inclined the substrates at 90° and observed that the drop remains hanging regardless of any substrate movements. Moreover, we flipped the ZnO substrate upside down at 180°, and the attachment of the drop was still observed. Thus, we believe that sliding angles may not exist in the hydrophobic ZnO nanorods substrates with high density of nanorods. Earlier studies[52,53] reported similar observations for the adhesion of the liquid drop on ZnO nanorods substrates.

Hydroxyl-Based Dissociation-Exchange Mechanism. Low surface tension aliphatic hydroxyl-based alcoholic HCs (*e.g.*, IPA, methanol, and ethanol) and double-bond oxygen-based structures (*e.g.*, acetone) showed very high wettability because of −OH and =O radicals with increasing GO hydrophilicity in water owing to the formed hydrogen bonds between water/organic. At the surface of ZnO nanorods, −OH groups are chemisorbed by the dissociation of alcohols at room temperature. Only hydrogen in the hydroxyl group of alcohol can be exchanged owing to the catalytic behavior of ZnO (Figure 5). ZnO acts as a catalyst to alcohol dehydrogenation that would facilitate the formation of zinc alcoholate compounds. The removed hydrogen atom bonds with the oxygen sites in the ZnO nanorod crystal forming surface hydroxyl groups.[54] The hypothesized wettability mechanism in detail can be summarized from combining and understanding

https://dx.doi.org/10.1021/acsami.0c09559
ACS Appl. Mater. Interfaces 2020, 12, 39772−39780

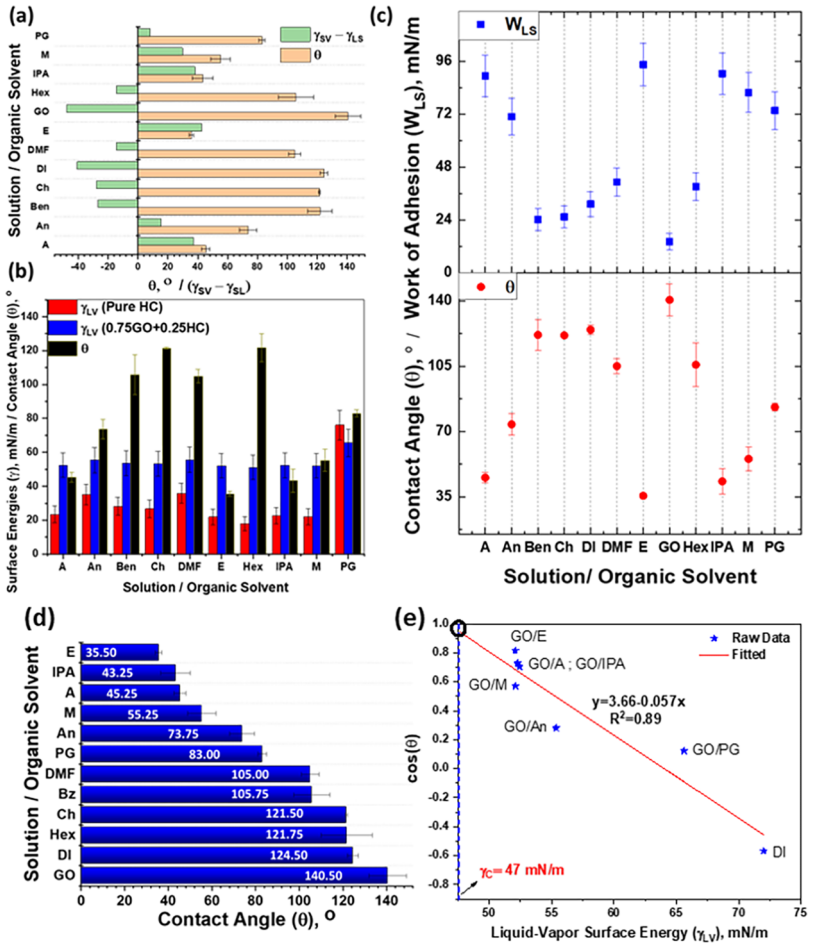

Figure 4. Wettability analysis and results of GO-coated ZnO nanorods obtained from Young and Young–Dupre models: (a) contact angle and its relationship with ($\gamma_{SV} - \gamma_{LS}$) for GO–water and GO–water mixed with different organics; (b) liquid–vapor surface energy (γ_{LV}) in GO–water and GO–water/organics mixture and its impact on the wettability contact angle; (c) symmetric behavior obtained between work of adhesion (W_{LS}) *vs* contact angle, indicating the inverse correlation; (d) mixed GO–water/organic solutions *vs* measured experimental contact angles; and (e) Fox–Zisman linear approximation showing the critical surface tension (γ_c) necessary for complete wettability.

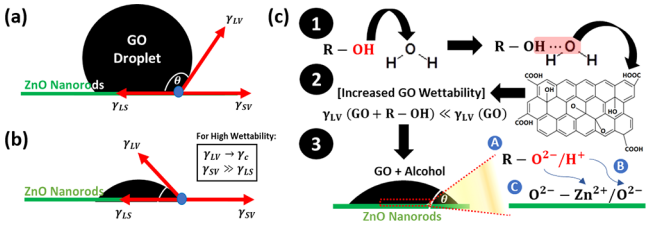

Figure 5. Observed wettability angles on ZnO nanorods for (a) GO–water suspensions; (b) GO–water/alcohol or GO–water/acetone-mixed solutions; and (c) hypothesized mechanism of wettability for alcohol/water in (1) from formed hydrogen bonds interacting with GO functional groups in (2), reducing the overall γ_{LV} and lowering liquid–solid contact angle in (3) on ZnO nanorods for GO mixed with alcoholic compounds: (A) dehydrogenation of alcohol; (B) hydrogen bond formation; and (C) formation of possible zine alcoholate compounds.

possible interactions and bonding mechanisms found in the previous literature[54,55] (Figure 5):

1. GO becomes more wettable in the water suspension because of the formed hydrogen bonds between water/organic from the introduced hydroxyl and carboxyl groups in organics.
2. Liquid–vapor surface energy of GO–water/organic becomes less than that of GO–water contributing in lowering contact angle of the casted GO droplet on the ZnO substrate.
3. ZnO has high affinity to organics (alcohols) and attracts hydroxyl/carboxyl groups present in GO–water/organic suspensions; hence, dipole–dipole interactions or possible hydrogen bonds might exist between [H^+ dehydrogenated from functional groups in (GO/organic)] and (O^{2-} in ZnO) providing a high work of adhesion with increased ZnO wettability:
    a. Dehydrogenation of −OH (hydroxyl groups) present in the alcoholic structure.
    b. Formation of O···H hydrogen bonds at the interface connecting O^{2-} in the ZnO to H^+ in the organic structure (from the catalytic dehydrogenation reaction).
    c. Formation of possible zinc alcoholate compounds between Zn^{2+} and O^{2-} in the organic alcohol.

To ensure the existence of the synthesized ZnO nanorods and understand the impact of organophilicity of GO on interfacing GO with ZnO nanorods, Fourier transform infrared (FT-IR) spectra of the synthesized ZnO nanorods, ZnO nanorods interfaced with GO, and ZnO nanorods interfaced

https://dx.doi.org/10.1021/acsami.0c09559
ACS Appl. Mater. Interfaces 2020, 12, 39772–39780

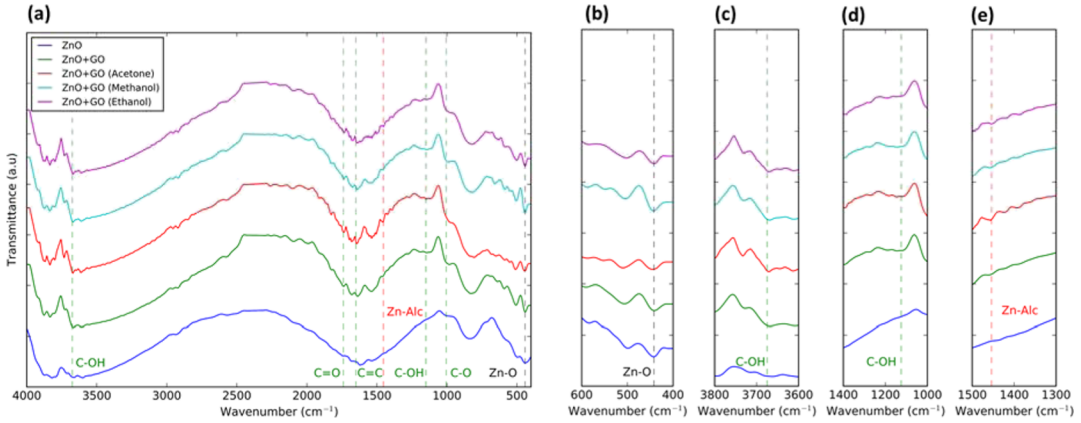

Figure 6. (a) Full FT-IR spectra of ZnO and ZnO interfaced with GO suspended in different organic solvents. (b–e) Zoomed-in spectra showing Zn–O and C–OH stretching behavior in different samples and formation of zinc alcoholate in GO-coated ZnO heterostructures.

with GO mixed with different organic solvents (*e.g.*, acetone, methanol, and ethanol) were recorded, as shown in Figure 6. All of the analyzed samples show the characteristic Zn–O stretching[56,57] at ∼442 cm^{-1} and a shoulder at ∼500 cm^{-1}, as can be seen from Figure 6b confirming the presence of ZnO nanorods. Figure 6a shows the characteristic C═O (∼1740 cm^{-1}), C═C (∼1650 cm^{-1}), and C–O (∼1005 cm^{-1}) stretching peaks[58,59] from GO on ZnO, which are shifted by +19 cm^{-1}, +29 cm^{-1}, and −43 cm^{-1}, respectively, as compared to free GO.[60] The observed shifts in C═O and C═C peaks are because of GO interactions with ZnO. These signature peaks are absent from the pure ZnO spectrum (blue color bottom spectrum). Zoomed-in spectra shown in Figure 6c,d indicate the presence of C–OH modes from the hydroxyl groups of GO from the basal plane and the sheet edges at ∼3675 and ∼1150 cm^{-1}, respectively.[61,62] Because the intensity of Zn–O stretching bands is similar in all the samples, it can be hypothesized that the intensity of C–OH stretching bands can suggest interactions of ZnO with GO. This is quantified in Table 2 as the ratio of peak intensities of C–OH stretching to Zn–O stretching. ZnO interfaced with GO has significantly higher ratios when suspended in acetone, methanol, and ethanol compared to just when it is suspended in water. The higher ratio is a qualitative indication of more interactions with the solvents and, therefore, of higher organophilicity of GO for better ZnO wettability. This observation further confirms the proposed dipole–dipole interactions or possible hydrogen bonding between GO–water/organic suspensions and ZnO. The C–OH stretching is believed to become stronger with solvents because of the created O···H hydrogen bonds between water and the solvent, GO and the solvent, or GO/organic [H^+] and ZnO [O^{2-}], which altogether would increase the ZnO wettability.

Table 2. FT-IR Peak Intensity Ratios of the C–OH Stretching Mode of the Interfaced GO to the Zn–O Stretching Mode of ZnO

sample	C–OH/Zn–O[a]	C–OH/Zn–O[b]
ZnO + GO	0.38	3.48
ZnO + GO acetone	0.89	5.96
ZnO + GO methanol	0.62	3.90
ZnO + GO ethanol	0.61	4.63

[a]C–OH mode at ∼3675 cm^{-1}. [b]C–OH mode at ∼1150 cm^{-1}.

Interfacial interactions between the organic and ZnO nanorods further confirm the formation of zinc alcoholate compounds at the interface due to the observed mode at ∼1454 cm^{-1} in the zoomed-in spectra, as shown in Figure 6e.

Overall, it is determined that regardless of the organic compound used, the interfacing of graphene to ZnO is still achieved. This can possibly be explained by the interaction of metal oxides with both water and organics. Earlier studies showed that despite being hydrophobic, ZnO is very adsorbent to alcohols. A previous study[55] showed that when there are no hydroxyl groups present at the ZnO surface, the metal oxide has the highest volume of alcohol adsorption. We believe that the proposed dissociation-exchange mechanism is effective to possibly introduce strong interfacial interactions between GO and ZnO responsible for the enhancement of ZnO surface wettability toward GO. The revealed high work of adhesion estimated when adding certain organics (*e.g.*, methanol, ethanol, acetone, and IPA) confirms this high wettability, which also results from the reduced liquid–vapor surface energy of GO–water suspensions, according to Table S2 in the Supporting Information and Figure 4b. This provides many advantages over the other means (to increase ZnO wettability), including scalability, cost-effectiveness, easy processability, and possibility to produce well-interfaced GO layers/ZnO nanorods heterostructures.

CONCLUSIONS

In summary, we have presented a "hydroxyl-based dissociation-exchange" mechanism for designing mixed-dimensional GO layer-coated ZnO nanorods heterostructures. First, a decrease in the liquid–vapor surface tension (γ_{LV}) of the GO–water/organic droplet is achieved because of the organophilicity of GO from strong hydrogen bond interactions with hydroxyl/carboxyl radicals. Second, a high affinity toward drop-casted GO–water suspension arises when alcohol-based media are introduced demonstrating enhanced ZnO nanorods chemisorption and therefore wettability (decrease in γ_{LS}). The combination of these two processes is believed to result in the sharp reduction of the contact droplet angle on ZnO nanorods, with a volumetric ratio of 1:3 (organic-to-GO), showing as high as 75% reduction in the contact angle (θ = 35.5°) with the addition of alcohols. The proposed method leverages a scalable technique for developing graphene–ZnO heterojunctions; opening avenue for interfacing wide band gap

https://dx.doi.org/10.1021/acsami.0c09559
ACS Appl. Mater. Interfaces 2020, 12, 39772–39780

semiconductors with graphene for future optoelectronic and biosensing applications.

MATERIALS AND METHODS

Zn Foil Substrate Preparation. Zn foil (200 μm thick) was purchased from US Sigma-Aldrich and cut into 1 cm^2 squares. The Zn substrates are then sonicated for 15 min in acetone and then another 15 min in IPA to ensure a clean surface prior the growth step. After sonication, the samples are blow dried and prepped for annealing. The substrates are then annealed in a vacuum furnace for 2 h at 150 °C with a pressure of 1×10^{-4} Pa for crystallization and reduced grain boundaries. After annealing, one side of the Zn substrate is scored with a diamond cutter to distinguish the backside that is coated later with a poly-methyl methacrylate (PMMA) layer. For backside PMMA coating, the Zn foils are placed on a spin coater (3000 rpm) to prevent the growth of ZnO nanorods on the backside and have uniform coating on the frontside. The PMMA coating process is repeated up to three times to ensure a proper layer formation. The PMMA-coated Zn foils are left to dry overnight under a laminar hood.

ZnO Hydrothermal Growth Solution. The final solution that is to be used is a blend of two separate mixtures. The first is a mixture of zinc acetate dihydrate [$Zn(CH_3CO_2)_2{\cdot}2H_2O$] and DI water, with a concentration of 25 mM; the other mixture of 50 mM is prepared using DI water and hexamine [$(CH_2)_6N_4$] [*i.e.*, 1:2 concentration ratio of $Zn(CH_3CO_2)_2{\cdot}2H_2O$ to $(CH_2)_6N_4$]. The solutions are then mixed with a stirrer in a large beaker and then heated to 60 °C and stirred for 15 min to have a clear solution. The prepared solution is then poured in a lined-up Teflon container. The container is placed in an autoclave and kept in an oven to initiate the reaction. The growth reaction takes place for 4 h at 90 °C for optimal growth. After 4 h, the autoclave is removed from the oven and placed on a countertop to cool for 15 min. Once cooled, the Teflon container is removed, and the solution is drained for sample extraction. The sample is carefully taken out and placed onto a Petri dish and left to dry overnight at room temperature in the laminar hood. A white layer of the metal oxide is observed, indicating formation of ZnO nanorods on the Zn foil. For the hydrophobicity study, the sample is cut into four pieces to repeat contact angle measurements more than three times for accuracy of the results.

Synthesis of GO Suspension. A GO/DI suspension is synthesized using the modified Hummers method, as reported in previous works.[63−65] Briefly, we initiated GO synthesis by mixing 1 g of graphite powders with 0.5 g of sodium nitrate ($NaNO_3$) in a 23 mL of concentrated sulfuric acid (H_2SO_4). Addition of 6 g of potassium permanganate ($KMnO_4$) as an oxidizing agent to the suspension is carried out subsequently under continuous stirring and ice-bath cooling for 1 h to maintain the suspension below room temperature (~0 °C). The mixture is then stirred for 12 h at 35 °C until the suspension became dark green. The exothermic reaction is then terminated (the excess $KMnO_4$ is also eliminated) by the addition of 500 mL of DI water and 3 mL of 30% hydrogen peroxide (H_2O_2). Undesired ions/particulates are removed through washing the suspension with a 1:10 hydrochloric acid (HCl) to DI water (25:250 mL) and then dialyzed at room temperature (~23 °C) in a DI bath overnight, while changing the DI water every 1 h during the first 6 h to remove undesirable metal ions, acids, and other functional groups responsible for the high suspension acidity.[63] The resultant GO suspension become much pure with a low acidity (pH ~ 6) owing to the elimination of acidic ions from the produced mixture (without addition of sodium hydroxide or any other hydroxyl ions to the suspension). The pH of the GO suspension plays a key role in determining the feasibility of interfacing 2D GO with 1D ZnO nanorods because it is believed that high suspension acidity may result in degrading the ZnO substrate and impacting the wettability analysis.

HC Medium Used for Dispersing GO/DI Suspensions in the Wettability Study. Ten different HC chemicals (organic medium) are selected as prospective media for GO (organics: acetone [>99.8%], IPA [>99.5%], methanol [>99.8%], ethanol [>95%], anisol [>99%], polyethylene glycol [>50% in H_2O], DMF [>99.8%], benzene [>99.8%], hexane [>95%], and chloroform [>99%]). It is hypothesized that the existing organic functional groups should have an impact on the wettability properties of GO when interfaced with the presynthesized 1D ZnO nanorods. All chemicals are of laboratory grade and are used as received (without prior treatments) for our wettability analysis. For comparison purposes, pure suspensions of GO and DI are tested prior to initiating the mixing process with HCs to check the original wettability contact angles of ZnO substrates to GO and/or DI.

FT-IR Characterization. The FT-IR spectra were recorded on a Bruker Invenio S FT-IR spectrometer using the transmission mode on a custom 3D printed sample holder at a resolution of 4 cm^{-1}. Each tested sample was approximately 5 mm × 5 mm. Hence, the beam diameter was adjusted to be 7 mm to ensure that the sample was in the beam path. A low sampling rate of 7.5 kHz was used to enhance the signal-to-noise ratio of the spectra. Spectra for each sample were averaged over 70 scans and were compensated for the presence of atmospheric CO_2.

ASSOCIATED CONTENT

Supporting Information

The Supporting Information is available free of charge at https://pubs.acs.org/doi/10.1021/acsami.0c09559.

Contact angle and wettability relationship; liquid−vapor surface tension (γ_{LV}) of various liquids and organic solvents (either γ_{GO} or γ_{HC}) with air; mechanisms and chemical reactions involved in the growth and synthesis of ZnO nanorods; apparatus for the contact angle measurement; and confocal Raman spectroscopy analysis of DI/ZnO and GO/ZnO heterostructure films using different solvents (PDF)

AUTHOR INFORMATION

Corresponding Authors

Dieter M. Gruen − *Dimerond Technologies, LLC, Downers Grove, Illinois 60516, United States*; Email: dietergruen@comcast.net

Vikas Berry − *Department of Chemical Engineering, University of Illinois at Chicago, Chicago, Illinois 60607, United States*; orcid.org/0000-0002-1102-1996; Email: vikasb@uic.edu

Sanjay K. Behura − *Department of Chemical Engineering, University of Illinois at Chicago, Chicago, Illinois 60607, United States*; orcid.org/0000-0001-7339-9997; Email: sbehura1@uic.edu

Authors

Pavan S. Emani − *Department of Civil and Materials Engineering, University of Illinois at Chicago, Chicago, Illinois 60607, United States*

Hisham A. Maddah − *Department of Chemical Engineering, University of Illinois at Chicago, Chicago, Illinois 60607, United States; Department of Chemical Engineering, King Abdulaziz University, Rabigh 21911, Saudi Arabia*; orcid.org/0000-0002-8208-8629

Arjun Rangoonwala − *Department of Chemical Engineering, University of Illinois at Chicago, Chicago, Illinois 60607, United States*

Songwei Che − *Department of Chemical Engineering, University of Illinois at Chicago, Chicago, Illinois 60607, United States*

Aditya Prajapati − *Department of Chemical Engineering, University of Illinois at Chicago, Chicago, Illinois 60607, United States*

https://dx.doi.org/10.1021/acsami.0c09559
ACS Appl. Mater. Interfaces 2020, 12, 39772−39780

Meenesh R. Singh − *Department of Chemical Engineering, University of Illinois at Chicago, Chicago, Illinois 60607, United States;* orcid.org/0000-0002-3638-8866

Complete contact information is available at: https://pubs.acs.org/10.1021/acsami.0c09559

Author Contributions

⊥P.S.E. and H.A.M. equal contributions.

Notes

The authors declare no competing financial interest.

■ ACKNOWLEDGMENTS

S.K.B. and V.B. thank Dimerond Technologies, LLC for the support to conduct renewable energy research at the University of Illinois at Chicago. All of the authors thank the University of Illinois at Chicago for the support. H.A.M. would like to acknowledge the Saudi Arabian Cultural Mission (SACM) and King Abdulaziz University (KAU) for their support and funding to pursue the graduate studies. S.C. acknowledges the use of FESEM at Center for Nanoscale Materials at Argonne National Laboratory. V.B. thanks funding support from the National Science Foundation (grant: 1054877) and Office of Naval Research (grants: N000141110767 and N000141812583).

■ REFERENCES

(1) Behura, S. K.; Wang, C.; Wen, Y.; Berry, V. Graphene−Semiconductor Heterojunction Sheds Light on Emerging Photovoltaics. *Nat. Photonics* **2019**, *13*, 312.

(2) Behura, S.; Chang, K.-C.; Wen, Y.; Debbarma, R.; Nguyen, P.; Che, S.; Deng, S.; Seacrist, M. R.; Berry, V. WS2/Silicon Heterojunction Solar Cells: A CVD Process for the Fabrication of WS2 Films on p-Si Substrates for Photovoltaic and Spectral Responses. *IEEE Nanotechnol. Mag.* **2017**, *11*, 33−38.

(3) Lin, J.; Penchev, M.; Wang, G.; Paul, R. K.; Zhong, J.; Jing, X.; Ozkan, M.; Ozkan, C. S. Heterogeneous Graphene Nanostructures: Zno Nanostructures Grown on Large-Area Graphene Layers. *Small* **2010**, *6*, 2448.

(4) Al-Hossainy, A. F.; Zoromba, M. S.; Abdel-Aziz, M. H.; Bassyouni, M.; Attar, A.; Zwawi, M.; Abd-Elmageed, A. A. I.; Maddah, H. A.; Ben Slimane, A. Fabrication of Heterojunction Diode Using Doped-Poly (Ortho-Aminophenol) for Solar Cells Applications. *Phys. B* **2019**, *566*, 6.

(5) Arya, S. K.; Saha, S.; Ramirez-Vick, J. E.; Gupta, V.; Bhansali, S.; Singh, S. P. Recent Advances in ZnO Nanostructures and Thin Films for Biosensor Applications: Review. *Anal. Chim. Acta* **2012**, *737*, 1−21.

(6) Fu, Y. Q.; Luo, J. K.; Du, X. Y.; Flewitt, A. J.; Li, Y.; Markx, G. H.; Walton, A. J.; Milne, W. I. Recent Developments on ZnO Films for Acoustic Wave Based Bio-Sensing and Microfluidic Applications: A Review. *Sens. Actuators, B* **2010**, *143*, 606.

(7) Zhao, Z.; Lei, W.; Zhang, X.; Wang, B.; Jiang, H. ZnO-Based Amperometric Enzyme Biosensors. *Sensors* **2010**, *10*, 1216.

(8) Xue, Y.; Liu, J.; Chen, H.; Wang, R.; Li, D.; Qu, J.; Dai, L. Nitrogen-Doped Graphene Foams as Metal-Free Counter Electrodes in High-Performance Dye-Sensitized Solar Cells. *Angew. Chem., Int. Ed.* **2012**, *51*, 12124.

(9) Panda, S. K.; Jacob, C. Preparation of Transparent ZnO Thin Films and Their Application in UV Sensor Devices. *Solid-State Electron.* **2012**, *73*, 44.

(10) Vittal, R.; Ho, K.-C. Zinc Oxide Based Dye-Sensitized Solar Cells: A Review. *Renewable Sustainable Energy Rev.* **2017**, *70*, 920.

(11) Karki, I. B.; Nakarmi, J. J.; Mandal, P. K.; Chatterjee, S. Effect of Organic Dyes on the Performance of ZnO Based Dye-Sensitized Solar Cells. *Appl. Sol. Energy* **2013**, *49*, 40.

(12) Maddah, H. A.; Berry, V.; Behura, S. K. Biomolecular Photosensitizers for Dye-Sensitized Solar Cells: Recent Developments and Critical Insights. *Renewable Sustainable Energy Rev.* **2020**, *121*, 109678.

(13) Yao, X.; Liang, J.; Li, T.; Fan, L.; Shi, B.; Wei, C.; Ding, Y.; Li, Y.; Zhao, Y.; Zhang, X. Electron Transport Layer Driven to Improve the Open-Circuit Voltage of CH 3 NH 3 PbI 3 Planar Perovskite Solar Cells. *Sci. China Mater.* **2018**, *61*, 65.

(14) Pistor, P.; Ruiz, A.; Cabot, A.; Izquierdo-Roca, V.; Fu, Q.; Tang, X.; Huang, B.; Hu, T.; Tan, L.; Chen, L.; et al. Advanced Raman Spectroscopy of Methylammonium Lead Iodide: Development of a Non-destructive Characterisation Methodology. *Adv. Sci.* **2016**, *6*, 35973.

(15) Maddah, H. A.; Berry, V.; Behura, S. K. Cuboctahedral Stability in Titanium Halide Perovskites via Machine Learning. *Comput. Mater. Sci.* **2020**, *173*, 109415.

(16) Lonkar, S. P.; Pillai, V.; Abdala, A. Solvent-Free Synthesis of ZnO-Graphene Nanocomposite with Superior Photocatalytic Activity. *Appl. Surf. Sci.* **2019**, *465*, 1107−1113.

(17) Xue, B.; Zou, Y. High Photocatalytic Activity of ZnO−Graphene Composite. *J. Colloid Interface Sci.* **2018**, *529*, 306−313.

(18) Ameen, S.; Akhtar, M. S.; Song, M.; Shin, H. S. Vertically Aligned ZnO Nanorods on Hot Filament Chemical Vapor Deposition Grown Graphene Oxide Thin Film Substrate: Solar Energy Conversion. *ACS Appl. Mater. Interfaces* **2012**, *4*, 4405.

(19) Joshi, B. N.; Yoon, H.; Na, S.-H.; Choi, J.-Y.; Yoon, S. S. Enhanced Photocatalytic Performance of Graphene-ZnO Nanoplatelet Composite Thin Films Prepared by Electrostatic Spray Deposition. *Ceram. Int.* **2014**, *40*, 3647.

(20) Zhang, J.; Tan, T.; Zhao, Y.; Liu, N. Preparation of ZnO Nanorods/Graphene Composite Anodes for High-Performance Lithium-Ion Batteries. *Nanomaterials* **2018**, *8*, 966.

(21) Huang, L.; Guo, G.; Liu, Y.; Chang, Q.; Shi, W. Synthesis of Reduced Graphene Oxide/ZnO Nanorods Composites on Graphene Coated PET Flexible Substrates. *Mater. Res. Bull.* **2013**, *48*, 4163.

(22) Rawat, K.; Sharma, A.; Solanki, P. R.; Bohidar, H. B. Potential of Gelatin-Zinc Oxide Nanocomposite as Ascorbic Acid Sensor. *Electroanalysis* **2015**, *27*, 2448.

(23) Qurashi, A.; Subrahmanyam, K. S.; Kumar, P. Nanofiller Graphene-ZnO Hybrid Nanoarchitecture: Optical, Electrical and Optoelectronic Investigation. *J. Mater. Chem. C* **2015**, *3*, 11959−11964.

(24) He, G.; Wang, K. The Super Hydrophobicity of ZnO Nanorods Fabricated by Electrochemical Deposition Method. *Appl. Surf. Sci.* **2011**, *257*, 6590−6594.

(25) Khranovskyy, V.; Ekblad, T.; Yakimova, R.; Hultman, L. Surface Morphology Effects on the Light-Controlled Wettability of ZnO Nanostructures. *Appl. Surf. Sci.* **2012**, *258*, 8146.

(26) Bhavsar, K.; Prabhu, R.; Pollard, P. Investigations on Surface Wettability of ZnO Nanowires Using UV LEDs for Biosensing Applications. *IOP Conference Series: Materials Science and Engineering*, 2014.

(27) Myint, M. T. Z.; Kumar, N. S.; Hornyak, G. L.; Dutta, J. Hydrophobic/Hydrophilic Switching on Zinc Oxide Micro-Textured Surface. *Appl. Surf. Sci.* **2013**, *264*, 344.

(28) Xu, K.; Zhang, J.; Hao, X.; Zhang, C.; Wei, N.; Zhang, C. Wetting Properties of Defective Graphene Oxide: A Molecular Simulation Study. *Molecules* **2018**, *23*, 1439.

(29) Shih, C.-J.; Lin, S.; Sharma, R.; Strano, M. S.; Blankschtein, D. Understanding the PH-Dependent Behavior of Graphene Oxide Aqueous Solutions: A Comparative Experimental and Molecular Dynamics Simulation Study. *Langmuir* **2012**, *28*, 235.

(30) Maddah, H. A. Adsorption Isotherm of NaCl from Aqueous Solutions onto Activated Carbon Cloth to Enhance Membrane Filtration. *J. Appl. Sci. Eng.* **2020**, *23*, 69 DOI: 10.6180/jase.202003_23(1).0009.

(31) Nunes, V. M. B. Surface and Interface Chemistry: Liquid/gas Interface https://slideplayer.com/slide/8283779/.

(32) Eral, H. B.; 't Mannetje, D. J. C. M.; Oh, J. M. Contact Angle Hysteresis: A Review of Fundamentals and Applications. *Colloid Polym. Sci.* **2013**, *291*, 247.
(33) Johnson, E. PHASE OF MATTER: The Elusive Liquid-Solid Interface. *Science* **2002**, *296*, 477−478.
(34) Liu, B.; Zeng, H. C. Hydrothermal Synthesis of ZnO Nanorods in the Diameter Regime of 50 Nm. *J. Am. Chem. Soc.* **2003**, *125*, 4430−4431.
(35) Pourshaban, E.; Abdizadeh, H.; Golobostanfard, M. R. ZnO Nanorods Array Synthesized by Chemical Bath Deposition: Effect of Seed Layer Sol Concentration. *Procedia Mater. Sci.* **2015**, *11*, 352−358.
(36) Shi, R.; Yang, P.; Dong, X.; Ma, Q.; Zhang, A. Growth of Flower-like ZnO on ZnO Nanorod Arrays Created on Zinc Substrate through Low-Temperature Hydrothermal Synthesis. *Appl. Surf. Sci.* **2013**, *264*, 162−170.
(37) Parize, R.; Garnier, J.; Chaix-Pluchery, O.; Verrier, C.; Appert, E.; Consonni, V. Effects of Hexamethylenetetramine on the Nucleation and Radial Growth of ZnO Nanowires by Chemical Bath Deposition. *J. Phys. Chem. C* **2016**, *120*, 5242−5250.
(38) Shinde, S. S.; Bhosale, C. H.; Rajpure, K. Y. Photoelectrochemical Properties of Highly Mobilized Li-Doped ZnO Thin Films. *J. Photochem. Photobiol., B* **2013**, *120*, 1−9.
(39) Bhunia, A. K.; Jha, P. K.; Rout, D.; Saha, S. Morphological Properties and Raman Spectroscopy of ZnO Nanorods. *J. Phys. Sci.* **2016**, *21*, 2350−0352.
(40) Zhang, R.; Yin, P.-G.; Wang, N.; Guo, L. Photoluminescence and Raman Scattering of ZnO Nanorods. *Solid State Sci.* **2009**, *11*, 865−869.
(41) Yasri, N. G.; Sundramoorthy, A. K.; Chang, W.-J.; Gunasekaran, S. Highly Selective Mercury Detection at Partially Oxidized Graphene/Poly(3,4-Ethylenedioxythiophene):Poly(Styrenesulfonate) Nanocomposite Film-Modified Electrode. *Front. Mater.* **2014**, *1*, 33.
(42) Fu, Y.-X.; He, Z.-X.; Mo, D.-C.; Lu, S.-S. Thermal Conductivity Enhancement of Epoxy Adhesive Using Graphene Sheets as Additives. *Int. J. Therm. Sci.* **2014**, *86*, 276.
(43) Fang, S.; Huang, D.; Lv, R.; Bai, Y.; Huang, Z.-H.; Gu, J.; Kang, F. Three-Dimensional Reduced Graphene Oxide Powder for Efficient Microwave Absorption in the S-Band (2-4 GHz). *RSC Adv.* **2017**, *7*, 25773.
(44) Childres, I.; Jauregui, L. A.; Park, W.; Cao, H.; Chen, Y. Raman Spectroscopy of Graphene and Related Materials. *New Dev. Photon Mater. Res.* **2013**, *1*, 403.
(45) Young, T. An Essay on the Cohesion of Fluids. *Proc. R. Soc. London* **1832**, *1*, 171.
(46) Hansen, F. K. *The Measurement of Surface Energy of Polymers by Means of Contact Angles of Liquids on Solid Surfaces. A Short Overview of Frequently Used Methods*; University of Oslo: Oslo, 2004.
(47) Zisman, W. A. Relation of the Equilibrium Contact Angle to Liquid and Solid Constitution. *Advances in Chemistry*; ACS Publications, 1964.
(48) Kwok, D. Y.; Neumann, A. W. Contact Angle Interpretation in Terms of Solid Surface Tension. *Colloids Surf., A* **2000**, *161*, 31.
(49) Zisman, W. A. Relation of the Equilibrium Contact Angle to Liquid and Solid Constitution. *Contact Angle, Wettability, and Adhesion*; American Chemical Society, 1964.
(50) Lamour, G.; Hamraoui, A.; Buvailo, A.; Xing, Y.; Keuleyan, S.; Prakash, V.; Eftekhari-Bafrooei, A.; Borguet, E. Contact Angle Measurements Using a Simplified Experimental Setup. *J. Chem. Educ.* **2010**, *87*, 1403.
(51) Brugnara, M. *ImageJ: Contact Angle* https://imagej.nih.gov/ij/plugins/contact-angle.html.
(52) Kim, S. B.; Lee, W. W.; Yi, J.; Park, W. I.; Kim, J.-S.; Nichols, W. T. Simple, Large-Scale Patterning of Hydrophobic ZnO Nanorod Arrays. *ACS Appl. Mater. Interfaces* **2012**, *4*, 3910.
(53) Ghannam, H.; Chahboun, A.; Turmine, M. Wettability of Zinc Oxide Nanorod Surfaces. *RSC Adv.* **2019**, *9*, 38289.
(54) Koga, O.; Onishi, T.; Tamaru, K. Adsorption and Decomposition of Isopropyl Alcohol over Zinc Oxide. Infrared and Kinetic Study. *J. Chem. Soc., Faraday Trans. 1* **1980**, *76*, 19.
(55) Nagao, M.; Morimoto, T. Adsorption of Alcohols on Zinc Oxide Surfaces. *J. Phys. Chem.* **1980**, *84*, 2054−2058.
(56) Djelloul, A.; Aida, M.-S.; Bougdira, J. Photoluminescence, FTIR and X-Ray Diffraction Studies on Undoped and Al-Doped ZnO Thin Films Grown on Polycrystalline α-Alumina Substrates by Ultrasonic Spray Pyrolysis. *J. Lumin.* **2010**, *130*, 2113.
(57) Uysal, I.; Severcan, F.; Evis, Z. Characterization by Fourier Transform Infrared Spectroscopy of Hydroxyapatite Co-Doped with Zinc and Fluoride. *Ceram. Int.* **2013**, *39*, 7727.
(58) Tan, L.-L.; Ong, W.-J.; Chai, S.-P.; Goh, B. T.; Mohamed, A. R. Visible-Light-Active Oxygen-Rich TiO2 Decorated 2D Graphene Oxide with Enhanced Photocatalytic Activity toward Carbon Dioxide Reduction. *Appl. Catal., B* **2015**, *179*, 160.
(59) Xu, J.; Wang, K.; Zu, S.-Z.; Han, B.-H.; Wei, Z. Hierarchical Nanocomposites of Polyaniline Nanowire Arrays on Graphene Oxide Sheets with Synergistic Effect for Energy Storage. *ACS Nano* **2010**, *4*, 5019.
(60) Chen, X.; Chen, B. Macroscopic and Spectroscopic Investigations of the Adsorption of Nitroaromatic Compounds on Graphene Oxide, Reduced Graphene Oxide, and Graphene Nanosheets. *Environ. Sci. Technol.* **2015**, *49*, 6181.
(61) Viinikanoja, A.; Kauppila, J.; Damlin, P.; Suominen, M.; Kvarnström, C. In Situ FTIR and Raman Spectroelectrochemical Characterization of Graphene Oxide upon Electrochemical Reduction in Organic Solvents. *Phys. Chem. Chem. Phys.* **2015**, *17*, 12115.
(62) Nasrollahzadeh, M.; Jaleh, B.; Jabbari, A. Synthesis, Characterization and Catalytic Activity of Graphene Oxide/ZnO Nanocomposites. *RSC Adv.* **2014**, *4*, 36713.
(63) Zaaba, N. I.; Foo, K. L.; Hashim, U.; Tan, S. J.; Liu, W. W.; Voon, C. H. Synthesis of Graphene Oxide Using Modified Hummers Method: Solvent Influence. *Procedia Eng.* **2017**, *184*, 469.
(64) Alam, S. N.; Sharma, N.; Kumar, L. Synthesis of Graphene Oxide (GO) by Modified Hummers Method and Its Thermal Reduction to Obtain Reduced Graphene Oxide (RGO)*. *Graphene* **2017**, *6*, 1−18.
(65) Guerrero-Contreras, J.; Caballero-Briones, F. Graphene Oxide Powders with Different Oxidation Degree, Prepared by Synthesis Variations of the Hummers Method. *Mater. Chem. Phys.* **2015**, *153*, 209.

https://dx.doi.org/10.1021/acsami.0c09559
ACS Appl. Mater. Interfaces 2020, 12, 39772−39780